Influence of nanosecond repetitively pulsed discharges on the stability of a swirled propane/air burner representative of an aeronautical combustor

Séverine Barbosa, Guillaume Pilla, Deanna Lacoste, Philippe Scouflaire, Sebastien Ducruix, Christophe O. Laux, Denis Veynante

PHILOSOPHICAL TRANSACTIONS A

rsta.royalsocietypublishing.org

Research

Cite this article: Barbosa S, Pilla G, Lacoste DA, Scouflaire P, Ducruix S, Laux CO, Veynante D. 2015 Influence of nanosecond repetitively pulsed discharges on the stability of a swirled propane/air burner representative of an aeronautical combustor. *Phil. Trans. R. Soc. A* **373**: 20140335.
http://dx.doi.org/10.1098/rsta.2014.0335

Accepted: 6 May 2015

One contribution of 14 to a theme issue 'Physics and chemistry of plasma-assisted combustion'.

Subject Areas:
particle physics

Keywords:
flame stabilization, lean premixed combustion, optical diagnostics, plasma-assisted combustion, nanosecond repetitively pulsed discharges

Author for correspondence:
S. Barbosa
e-mail: severine.barbosa@univ-amu.fr

†Present address: Université Aix-Marseille, CNRS, UMR 7343, IUSTI, 13453 Marseille Cédex 13, France.
‡Present address: IFP—Energies Nouvelles, 92852 Rueil-Malmaison Cédex, France.

THE ROYAL SOCIETY PUBLISHING

Influence of nanosecond repetitively pulsed discharges on the stability of a swirled propane/air burner representative of an aeronautical combustor

S. Barbosa[1,2,†], G. Pilla[1,2,‡], D. A. Lacoste[1,2], P. Scouflaire[1,2], S. Ducruix[1,2], C. O. Laux[1,2] and D. Veynante[1,2]

[1]CNRS, UPR 288 Laboratoire EM2C, and [2]École Centrale Paris, Grande Voie des Vignes, 92290 Chatenay-Malabry, France

This paper reports on an experimental study of the influence of a nanosecond repetitively pulsed spark discharge on the stability domain of a propane/air flame. This flame is produced in a lean premixed swirled combustor representative of an aeronautical combustion chamber. The lean extinction limits of the flame produced without and with plasma are determined and compared. It appears that only a low mean discharge power is necessary to increase the flame stability domain. Lastly, the effects of several parameters (pulse repetition frequency, global flowrate, electrode location) are studied.

1. Introduction

A convenient way to reduce NO*x* emissions in industrial combustion applications is to use lean premixed combustion. This consists in providing the combustion chamber with premixed reactants to avoid the formation of hot and fuel-rich pockets, which locally increase the NO*x* emissions.

In addition, under lean conditions, the mixture of fuel and air burns at lower temperature than for stoichiometric conditions, and therefore thermal NO*x* emissions are lower [1]. These conditions are generally

achieved in swirled lean premixed burners where the rotating flow both enhances the mixing rate between the fuel and the oxidizer streams and promotes the flame stabilization through the swirl-induced recirculation of hot products near the nozzle [2]. Unfortunately, strong instabilities may occur under these operating conditions and lead to mechanical damage and/or flame extinction [3,4]. Various solutions have already been proposed to improve and to control flame stabilization in these combustion chambers, from injector design improvements to complex adaptive active control methods.

Another way to improve flame stabilization is to use plasma discharges, which can generate active species and local heating sufficient to sustain the combustion of lean air/fuel mixtures. Over the past decade, for instance, beneficial effects have been observed in laboratory-scale burners under the action of microwave discharges [5], gliding arc discharges [6], plasma torches [7], surface DC discharges [8], nanosecond dielectric barrier discharges [9,10] or nanosecond repetitively pulsed (NRP) discharges [11–16]. The latter types of discharges have been particularly efficient, allowing the stabilization of lean premixed flames in laboratory-scale burners with plasma powers typically less than 1% of the power released by the flame. Thus, plasma-assisted combustion appears to be an effective and energy-efficient strategy for lean flame stabilization in well-controlled, laboratory-scale burners. However, few studies have been conducted in configurations close to practical systems.

In this study, we focus on the use of a non-equilibrium NRP discharge to increase the flame stability domain of a premixed swirled burner, representative of aeronautical combustors. The first objective of our work is to study the influence of a plasma discharge on the flame stability domain, particularly on the Lean Blow-Off (LBO) equivalence ratio. Then, the effects of the discharge repetition frequency, the flowrate and the relative electrode location in the combustor and the flame stability domain are investigated. The first part of this paper describes the experimental set-up: the combustor, the plasma device and the diagnostics used. Then, experimental results are presented and discussed.

2. Experimental set-up

(a) Experimental combustor

The experimental combustor is composed of a two-stage swirled injector and a rectangular combustion chamber with optical access ports. Figure 1 presents a schematic view of this experimental injector, whose geometry is relevant to that of industrial injectors.

A primary stage is used to facilitate ignition or to produce a pilot flame (fuel rich) in order to stabilize combustion. The primary stage comprises a central duct fed with pure propane and a swirler supplied with dry compressed air at ambient temperature. The angle of the primary stage swirler, containing 18 vanes, is maintained at 42°. Propane and air are mixed in a pipe downstream of the fuel and air inlets. The exit diameter of this primary stage nozzle is about 15 mm. The secondary stage is designed to dilute the propane/air mixture in order to obtain global lean conditions optimum for NOx emission reduction. In this secondary stage, propane is delivered through 15 holes, located on a circular hollow part. The airflow is injected in the secondary stage through a swirler with 20 vanes. The 15 propane jets mix with the secondary stage air flow in a cross-flow configuration. The angle of the secondary stage swirler is 35°.

Both swirlers are oriented in the same direction to ensure a strong co-rotating swirling motion. It has to be noted that both swirlers cannot be supplied with air independently of one another, i.e. the global incoming air flowrate is always divided into two parts. Because of the design of the two swirlers, the secondary stage air flowrate is always four times higher than the one in the primary stage. The maximum air flowrate that can be injected in the combustor is $Q_{\mathrm{air,max}} = 350\,\mathrm{Nm^3\,h^{-1}}$. Air and fuel mass flowrates are monitored with electronic mass flow meters and controllers (Bronkhorst-Elflow).

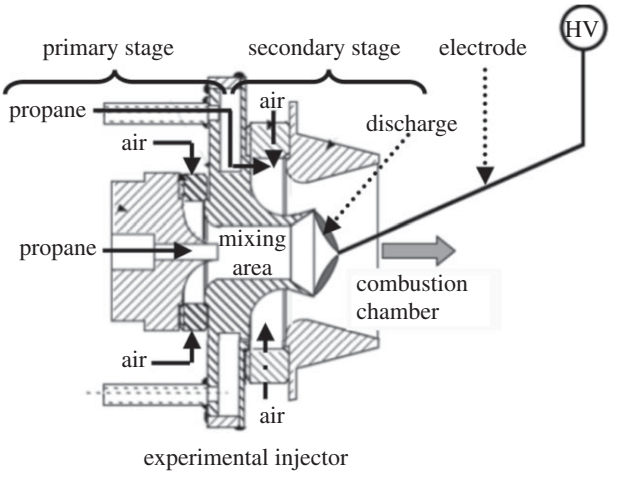

Figure 1. Schematic view of the experimental set-up and electrode locations.

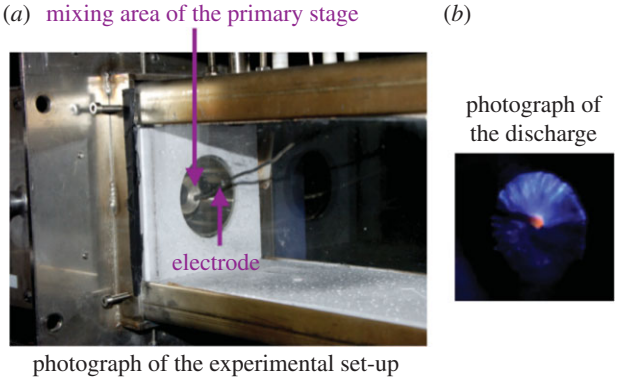

Figure 2. (*a*) The experimental set-up: combustion chamber, divergent outlet of the injector and electrode. (*b*) End view of the NRP discharge, taken with a digital camera equipped with a low-pass filter (03SWP604, Melles Griot; less than 450 nm). (Online version in colour.)

The combustion chamber has a square cross-section of $100 \times 100\,\mathrm{mm}^2$ and a length of 500 mm. The sidewalls of the chamber are made of two silica windows to enable optical diagnostics in the flame, whereas the top and the bottom walls of the chamber are made of concrete. The end of the combustion chamber is open to the atmosphere; therefore, the pressure at the end of the combustion chamber is close to atmospheric pressure.

(b) Plasma device

The plasma device includes a high-voltage pulse generator and a high-voltage electrode. A refractory steel anode, 5 mm in diameter, is introduced in the combustion chamber through its upper wall and is placed less than 1 cm downstream of the outlet of the primary stage mixing area, as shown in figures 1 and 2. The stainless steel nozzle, 55 mm in diameter, is used as the grounded cathode, and a discharge is created between the electrode tip and the edge of the injector outlet, as can be seen in figure 2. The photograph of the discharge shown in figure 2 is taken with a long time exposure, and therefore one can see several consecutive plasma filaments, each corresponding to a different pulse, almost uniformly distributed over the entire exit plane of the injector outlet. Plasma discharges are produced using a pulse generator (FID FPG 30-100MS).

Electric pulses of 10 ns in duration are created at the repetitive frequency $f_{30} = 30$ kHz, except for one test where the repetitive frequency is fixed at a value of $f_{11} = 11$ kHz to study the influence of this last parameter. The discharge operates in the nanosecond spark regime, as defined in [17–19] with peak currents of the order of 50 A during the 10 ns pulse. For the 30 kHz repetition frequency case, the peak voltage across the load is about 14 kV and the mean power provided by the discharge is about 350 W, to be compared with the flame power $P = 53$ kW (thus the plasma power is about 0.7% of the power released by the flame). For the 11 kHz case, the mean power delivered by the discharge is about 120 W.

(c) Optical diagnostics

The spontaneous optical emission of CH* and OH* radicals was recorded to evidence the enhancement of combustion by the discharge. CH* emission measurements were recorded with a digital camera (objective in conventional glass) equipped with a low-pass filter (03SWP604, Melles Griot; less than 450 nm), and OH* emission was measured with an intensified camera (Princeton Instrument PIMAX; 1 MHz) fitted with an interferential filter encompassing the OH* emission band (UG5, Melles Griot (210; 400 nm)). The two cameras were placed perpendicularly to the combustion chamber.

The choice of these optical diagnostics partly results from a previous study [11] in which the emission spectrum of a propane/air flame stabilized by an NRP discharge was measured between 300 and 500 nm under conditions similar to those in this study. The dominant emission features were found to be OH($A^2\Sigma^+ \rightarrow X^2\Pi$) around 310 nm, CH($A^2\Delta \rightarrow X^2\Pi$) around 430 nm, and various vibrational bands of the second positive system of N_2 ($C^3\Pi_u \rightarrow B^3\Pi_g$) between 300 and 500 nm. These measurements were taken over a time window of 1 ms encompassing the period of excitation by the 10 ns discharge. It is well known that the second positive system decays very quickly via dissociative quenching reactions: at atmospheric pressure the emission of the second positive system of N_2 decays by more than three orders of magnitude in less than 10 ns after the end of the discharge pulse [19]. In addition, it has to be remembered that the second positive system of N_2 is not visible outside the region where the discharge is produced. As the results shown in the following (figures 3 and 4) are taken downstream of the discharge region, the only observed emissions are from OH* between 300 and 320 nm, and CH* between 420 and 440 nm.

(d) Operating conditions

To investigate the effects of the plasma enhancement on the combustion process, all tests were performed with the same procedure. First, a flame was stabilized in the combustion chamber without plasma for given values of the air and fuel flowrates. Then the fuel flowrate was continuously decreased until flame extinction to determine the lean extinction equivalence ratio without plasma. Then, the same procedure was repeated to determine the lean equivalence ratio with plasma. As the fuel flowrate was significantly lower than the global air flowrate, a decrease in the fuel flowrate does not substantially modify the gas velocities in the combustion chamber. The influence of the global flowrate as well as the fuel injection location are studied at the end of this paper.

3. Influence of the plasma discharge on the flame stability domain

Our primary objective was to study the effects of NRP discharges (in the 30 kHz repetition frequency case) on the flame associated with the combustion regime labelled ‘case A’. For this study, the fuel was entirely injected through the primary stage, whereas the global airflow rate was kept constant at $Q_{air} = 105\,Nm^3\,h^{-1}$ (airflow rates in the primary and secondary stages: $(Q_{air})_p = 21\,Nm^3\,h^{-1}$ and $(Q_{air})_s = 84\,Nm^3\,h^{-1}$). In the following, as already mentioned, the associated flame extinction limit was determined by continuously reducing the fuel flowrate, i.e. the flame power, until flame extinction.

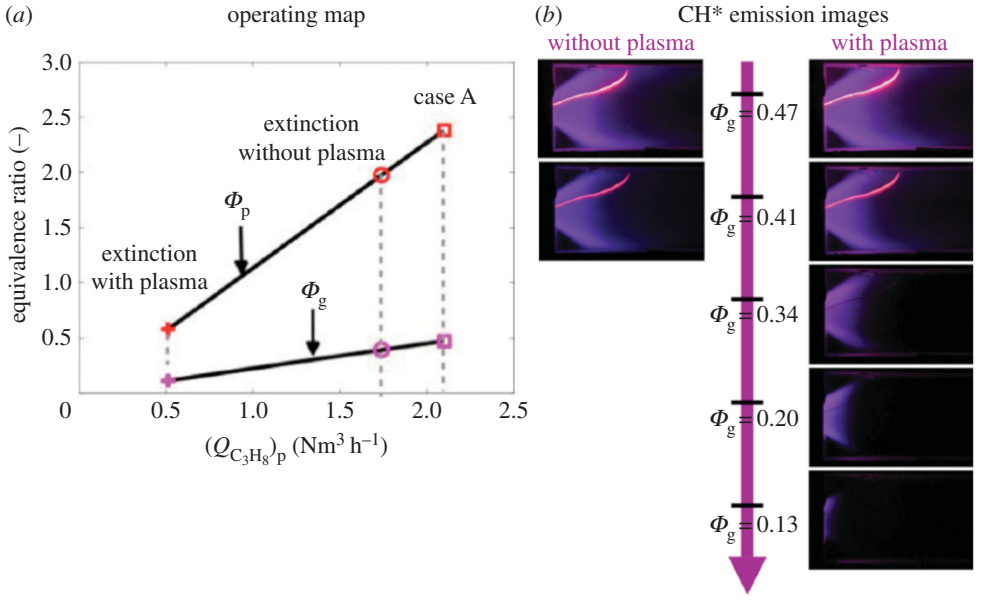

Figure 3. (*a*) Evolution of Φ_g (bottom) and Φ_p (top) as a function of $(Q_{C_3H_8})_p$. (*b*) CH* emission images obtained for $Q_{air} =$ 105 Nm^3 h^{-1} and for $(Q_{C_3H_8})_p < 2.1$ Nm^3 h^{-1} or $\Phi_g < 0.47$. The repetition rate of the discharge is 30 kHz. The bright filament visible in the photos is the anode heated by combustion gases. (Online version in colour.)

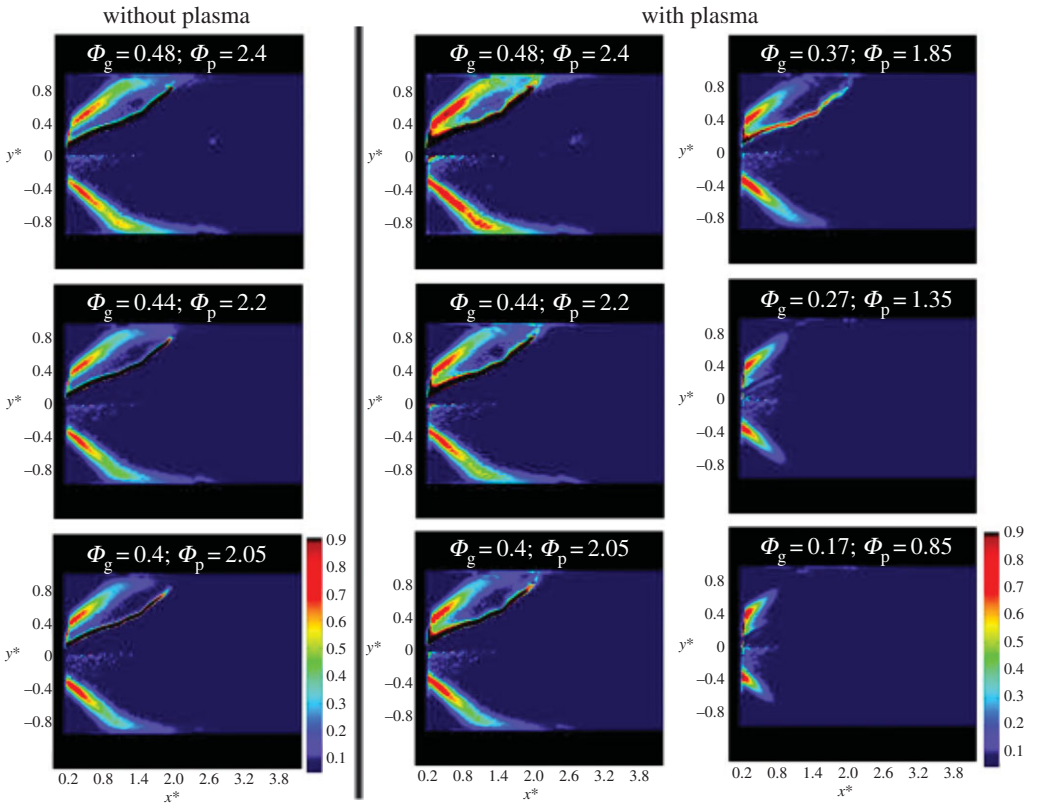

Figure 4. OH* emission images obtained for a constant air flowrate $Q_{air} = 105$ Nm^3 h^{-1} and a primary stage flowrate $(Q_{C_3H_8})_p$ of between 2.1 and 0.75 Nm^3 h^{-1} after Abel transform. (*a*) Flame without plasma enhancement. (*b*) Flame with plasma enhancement. (Online version in colour.)

(a) Flame stability domain without and with plasma

The operating regimes of the burner are determined as a function of the global equivalence ratio, Φ_g, the primary stage equivalence ratio, Φ_p, and the fuel flowrate, $(Q_{C_3H_8})_p$. Figure 3*a* shows the evolution of Φ_g and Φ_p when the fuel flowrate injected through the primary stage $(Q_{C_3H_8})_p$ decreases. As Q_{air} is kept constant, Φ_g and Φ_p decrease with $(Q_{C_3H_8})_p$. In figure 3*a*, the initial combustion regime for case A is represented by squares, the flame extinction limits without and with plasma are represented by circles and crosses, respectively. Without plasma, flame extinction is observed when the equivalence ratios are lower than $\Phi_g = 0.4$ and $\Phi_p = 2.05$, respectively. Note that the physical presence of the electrode (seen as the glowing filament in figure 3*b*) has no effect on the operation regimes, as flame extinction occurs at the same equivalence ratio with or without the electrode in the chamber. By contrast, when the plasma discharge is turned on, the lean equivalence ratios are reduced to $\Phi_g = 0.11$ and $\Phi_p = 0.57$, respectively. Thus, the plasma discharge significantly extends the flame stability domain, confirming the results already obtained in [11]. Here, the lean equivalence ratios are reduced by 72%. In addition, it must be noted that a flame is maintained when the primary stage gaseous mixture is lean: $0.57 < \Phi_p < 1$.

The operating map shown in figure 3*a* corresponds to different combustion regimes observed in the combustion chamber. They are analysed using CH^* emission images, reported in figure 3*b*. In both figures, emission images of the flame without plasma are plotted on the left and those of the flame with plasma enhancement are shown on the right. In these images, the flow goes from left to right.

The first two CH^* emission images show the flame observed in case A ($\Phi_g = 0.47$). Without and with plasma enhancement, the flame is compact and stabilized near the injection plane in the combustion chamber. The flame extends around the electrode, which is heated, becoming red. For a constant air flowrate, when Φ_g decreases from 0.47 to 0.4 the flame becomes shorter and more compact, but the plasma discharge does not alter the flame structure. Without plasma, when the global equivalence ratio is lower than 0.4, the flame extinguishes. Figure 3*b* indicates that the use of plasma allows a compact and robust flame to be maintained in the chamber even if $\Phi_g < 0.4$. For $\Phi_g < 0.34$, the flame becomes increasingly shorter so that the electrode is no longer in the flame and becomes invisible in the images. For $\Phi_g = 0.13$, the flame only develops around the end of the electrode, near the injection plane and in the injector outer divergent.

The frames in figure 4 were obtained by applying an Abel transform to the image recorded with the ICCD camera equipped with the interferential filters UG5. In all frames in figure 4, the locations of the top and the bottom walls of the combustion chamber are represented in black. The notations x^* and y^* are used to define reduced dimensions, $x^* = x/D$ and $y^* = y/D$, where D is the injector divergent outlet diameter ($D = 50$ mm). To ensure good image dynamics and reduce the effect of the highly luminous electrode, a threshold is applied to each image, which is then normalized by its maximum value. The image corresponding to $\Phi_g = 0.4$ and $\Phi_p = 2.05$ is representative of the flame near the extinction limit. For a constant air flowrate, reducing Φ_g from 0.47 to 0.4 makes the flame more compact and shorter. When Φ_g varies between 0.47 and 0.4, the level of OH^* emission is higher when the plasma discharge is applied to the flame.

In addition, for $\Phi_g = 0.4$, with plasma, the flame appears to be larger than in the case without plasma. When $\Phi_g < 0.4$, both the OH^* emission intensity and the flame length decrease. The combustion regime ($\Phi_g = 0.17$; $\Phi_p = 0.85$), close to the lean extinction limit ($\Phi_g = 0.11$; $\Phi_p = 0.57$), is a very short but very robust flame. Note that the phenomenon shown here is reversible: when Φ_g increases from 0.13, the same steps of the flame growth and development in the combustion chamber are observed.

4. Plasma discharge effectiveness

The influence of several parameters on the effectiveness of the plasma device in extending the lean extinction limit is now investigated.

Table 1. Lean extinction limits for case A. For these tests, the air flowrate is kept constant, $Q_{air} = 105\ Nm^3\ h^{-1}$. P is the power reached when the flame extinguishes.

		lean extinction		
	repetition frequency (Hz)	Φ_g	Φ_p	P (kW)
without plasma	—	0.4	2	44
with plasma	$f_{30} = 30$	0.11	0.55	13
with plasma	$f_{11} = 11$	0.34	1.7	38

(a) Influence of electric pulse repetition frequency

First, the effects of the electric pulse repetition frequency were determined. In the previous section, the case of a nanosecond plasma discharge with a repetition frequency $f_{30} = 30$ kHz was tested for the combustion regime termed 'case A'. The influence of a repetition frequency of $f_{11} = 11$ kHz is now analysed for the same combustion regime. The procedure is similar to that in the previous case: keeping the global air flowrate constant, the flame power is continuously decreased from $P = 53$ kW (by reducing the fuel flowrate) until flame extinction.

Table 1 reports the values of Φ_g and Φ_p when the flame extinguishes. Using an 11 kHz plasma discharge also allows us to increase the flame stability domain, since the lean extinction equivalence ratio decreases from ≈ 0.4 without plasma to ≈ 0.34 with plasma. Nevertheless, the results reported in table 1 evidence that the higher the repetition frequency, the more effective the plasma device is. Moreover, a stable flame with a primary stage equivalence ratio lower than unity, in contrast with the f_{30} case, cannot be maintained. For f_{11}, the plasma power is three times lower than the one obtained for f_{30}. This lower power may explain why the plasma device is less effective when its repetition frequency decreases.

(b) Influence of the global flowrate

Another important parameter to evaluate the effectiveness of the plasma device is the global flowrate (fuel + air) in the combustion chamber. Two complementary tests were performed using a plasma discharge pulsed at $f_{30} = 30$ kHz and the initial combustion regimes listed in table 2. For these two additional tests, the fuel flowrate was still injected only through the primary stage. These two tests are compared with case A. Cases A, B and C are characterized by close values of the global equivalence ratios but increasing flowrates, meaning that the initial fuel flowrate and the initial power are increased, as shown in table 2. Using the procedure described previously, the flame power is continuously decreased to determine the lean extinction limits. The latter are also reported in table 2.

As seen before, in case A, the plasma discharge provides a significant increase in the flame stability domain, as the lean extinction equivalence ratios are reduced by 72%. In case B, when the initial air flowrate is $Q_{air} = 122\ Nm^3\ h^{-1}$, the plasma discharge permits a very compact and robust flame to be obtained and the lean extinction equivalence ratios (Φ_g and Φ_p) to be reduced by 29% (table 2). Nevertheless, the analysis of case B indicates that the plasma device is less effective when the global flowrate increases. This is confirmed by the third case, where for $Q_{air} = 140\ Nm^3\ h^{-1}$ (case C) the lean extinction equivalence ratios are reduced by only 16% when the plasma device is used (table 2).

In conclusion, when the repetition frequency of the plasma discharge is kept constant, increasing the global flowrate in the combustion chamber reduces the effectiveness of the plasma device. These findings suggest that the residence time of the flow is a critical parameter, and that the repetition frequency of the plasma must be adjusted to ensure that the gas undergoes the influence of at least a few pulses. Another solution to maintain the discharge effectiveness

Table 2. Initial combustion regimes and lean extinction limits for cases A, B and C. Q_{air} and $(Q_{C_3H_8})_p$ are the air flowrate and the fuel flowrate (injected through the primary stage), respectively. Φ_g is the global equivalence ratio, Φ_p is the primary stage equivalence ratio and P is the burner power.

	Q_{air} (Nm^3 h^{-1})	$(Q_{C_3H_8})_p$ (Nm^3 h^{-1})	Φ_g	Φ_p	P (kW)
		initial combustion regimes			
case A	105	2.1	0.47	2.4	53
case B	122	2.4	0.47	2.3	60
case C	140	3	0.5	2.5	75
		lean extinction without plasma			
case A	105	1.76	0.4	2	44
case B	122	2.17	0.41	2.13	54
case C	140	2.5	0.43	2.15	63
		lean extinction with plasma			
case A	105	0.48	0.11	0.55	12
case B	122	1.5	0.29	1.47	37
case C	140	2.09	0.36	1.78	52

Table 3. Initial combustion regime and lean extinction limits for case D. $(Q_{C_3H_8})_s$ is the fuel flowrate in the secondary stage. Φ_s is the secondary stage equivalence ratio and P is the burner power.

	Q_{air} (Nm^3 h^{-1})	$(Q_{C_3H_8})_s$ (Nm^3 h^{-1})	Φ_g	Φ_s	P (kW)
case D	105	initial combustion regimes			
		2.9	0.66	0.82	74
		lean extinction without plasma			
		2.4	0.54	0.68	61
		lean extinction with plasma			
		2.3	0.52	0.66	59

would be to create a recirculation area (i.e. to increase the flow residence time) in the vicinity of the electrode.

(c) Influence of the electrode location

The relative position of the plasma discharge compared with the fuel injection probably also influences the flame stabilization using plasma. In other words, the local equivalence ratio of the gaseous mixture surrounding the electrode might have an important role for the plasma device effectiveness and is now investigated.

To this end, the fuel flowrate was totally injected through the secondary stage, without modifying the electrode location. The initial combustion regime is detailed in table 3. Note that the gaseous mixture exiting the secondary stage is a lean propane/air mixture; because of the injector geometry, the air flowrate in the secondary stage swirler is about four times higher than that in the primary stage swirler.

Once again, from the initial combustion regime (case D, initial flame power $P = 74$ kW), the flame power, i.e. the fuel flowrate, is continuously decreased until flame extinction, while Q_{air} is kept constant. In this case, the plasma discharge extends only slightly the flame stability domain: the lean extinction equivalence ratios are reduced by only 4% (table 3). In addition, this slight extension of the stability domain may only result from experimental errors. It should be noted that, in this case, the primary stage is only supplied with air. Thus, since the extremity of the electrode is placed on the axis of the primary stage mixing area, the discharge is produced in a pure airflow. As a result, the atomic oxygen produced by the discharge is likely to recombine before reaching the fuel. This may explain why the plasma device is not effective here. Nevertheless, further studies are required to optimize the electrode position in this configuration.

5. Conclusion

The effects of an NRP plasma on the flame stability domain of a lean premixed swirling burner were investigated. The plasma device provides high-voltage electric pulses with a peak voltage of 14 kV, a duration of 10 ns, and a repetition rate that can be adjusted in the range (1–100) kHz and a mean power of about 350 W.

We particularly focused on the influence of the plasma on the lean extinction limit. All tests were performed using the same procedure: for a constant airflow rate, and starting from a well-stabilized flame, the global equivalence ratio was decreased until flame extinction. The lean extinction equivalence ratio was then determined with and without discharge.

First, a plasma discharge with a repetitive frequency of 30 kHz was created on the combustion chamber axis near the divergent of the primary stage mixing area, while the burner power was ≈ 53 kW and the primary stage equivalence ratio was $\Phi_p = 2.4$. The use of the plasma discharge allowed us to stabilize the flame down to a lean extinction limit four times lower than without plasma. In addition, the plasma enhanced the combustion, leading to very short and compact flames when the global equivalence ratio was lower than the one associated with lean extinction when the plasma is off. This flame remains robust and is not subject to instabilities leading to extinction. Moreover, increasing the fuel flow rate in this situation leads back to a stable flame.

Then, the influence of several discharge parameters on the combustion effectiveness were investigated. This study confirms the conclusions of Pilla [20], i.e. that a key parameter is the repetition frequency, which must be high enough so that the discharge is in contact with a significant fraction of the gaseous reactive mixture present in the combustion chamber during a sufficient time. This comparison explains why, when the gas velocity increases, the repetition frequency of the discharge must be increased to improve the effectiveness of the discharge. Finally, the location of the electrodes is a key parameter. One must ensure that the discharge is produced in a region containing both air and fuel.

In conclusion, the use of NRP discharges allowed us to extend the stability domain of a lean premixed swirled injector representative of low-power aeronautical combustors, using an energy corresponding to a small fraction (0.7%) of the flame power. In future work, these plasma devices should be investigated in more powerful flames and/or combustors supplied with liquid fuels. In addition, the question of NO*x* emissions remains to be investigated. In flames stabilized by non-equilibrium discharges, separate studies have shown that the density of NO tends to remain constant when decreasing the equivalence ratio, at a level close to or slightly below the stoichiometric value [21,22]. This behaviour suggests that NO is formed by a non-thermal mechanism which could be the dissociative quenching of excited electronic levels of molecular nitrogen by the atomic oxygen produced in the discharge [23]. Further work is required to better understand this mechanism and to optimize the discharge electrical or geometrical parameters to effectively reduce NO production.

Data accessibility. All supporting data are included in the paper.

Authors' contributions. S.B. and G.P. designed the experiments and acquired the data. S.B. also analysed the data, drafted the manuscript and revised it critically. P.S. helped with the experiment. D.L. helped with the

experiment and manuscript revisions. S.D., D.V. and C.L. initiated and supervised the study, contributed to the manuscript and revised it critically. All authors give their final approval of the published version.

Competing interests. The authors have no competing interests related to this work.

Funding. S.B. and G.P. were supported by a PhD fellowship from Direction Générale de l'Armement (DGA). D.A.L., P.S., S.D. and D.V. are supported by CNRS. C.O.L. is supported by École Centrale Paris. Funding for the experiments was provided by the Initiative en Combustion Avancée (INCA programme) supported by SNECMA, DGA, ONERA and CNRS.

Acknowledgements. The authors would like to thank Dr Laurent Zimmer for his help with the OH imaging experiments.

References

1. Lefebvre AH. 1995 The role of fuel preparation in low-emission combustion. *J. Eng. Gas Turbines Power* **117**, 617–654. (doi:10.1115/1.2815449)
2. Syred N. 2006 A review of oscillation mechanisms and the role of the precessing vortex core (PVC) in swirl combustion systems. *Prog. Energy Combust. Sci.* **32**, 93–161. (doi:10.1016/j.pecs.2005.10.002)
3. Candel S. 2002 Combustion dynamics and control progress and challenges. *Proc. Combust. Inst.* **29**, 1–28. (doi:10.1016/S1540-7489(02)80007-4)
4. Nauert A, Peterson P, Linne M, Dreizler A. 2007 Experimental analysis of flashback in lean premixed swirling flames: conditions close to flashback. *Exp. Fluids* **43**, 89–100. (doi:10.1007/s00348-007-0327-x)
5. Esakov II, Grachev LP, Khodataev KV, Vinogradov VA, VanWie DM. 2006 Propane-air mixture combustion assisted by MW discharge in a speedy airflow. *IEEE Trans. Plasma Sci.* **34**, 2497–2506. (doi:10.1109/TPS.2006.886090)
6. Ombrello T, Qin X, Ju Y, Gutsol A, Fridman A, Carter C. 2006 Combustion enhancement via stabilized piecewise nonequilibrium gliding arc plasma discharge. *AIAA J.* **44**, 142–150. (doi:10.2514/1.17018)
7. Takita K. 2002 Ignition and flame-holding by oxygen, nitrogen, and argon plasma torches in supersonic airflow. *Combust. Flame* **128**, 301–313. (doi:10.1016/S0010-2180(01)00354-6)
8. Leonov SB, Kochetov IV, Napartovich AP, Sabelnikov VA, Yarantsev D. 2011 Plasma-induced ethylene ignition and flameholding in confined supersonic air flow at low temperatures. *IEEE Trans. Plasma Sci.* **39**, 781–787. (doi:10.1109/TPS.2010.2091512)
9. Mintoussov EI, Pancheshnyi SV, Starikovskii AY. 2004 Propane–air flame control by nonequilibrium low-temperature pulsed nanosecond barrier discharge. In *Proc. 42nd AIAA Aerospace Sciences Meeting and Exhibit, Reno, NV, 5–8 January 2004*, AIAA paper 2004-1013. Reston, VA: The American Institute of Aeronautics and Astronautics. (doi:10.2514/6.2004-1013)
10. Criner K, Cessou A, Louiche J, Vervisch P. 2006 Stabilization of turbulent lifted jet flames assisted by pulsed high voltage discharge. *Combust. Flame* **144**, 422–425. (doi:10.1016/j.combustflame.2005.09.010)
11. Pilla G, Galley D, Lacoste DA, Lacas F, Veynante D, Laux CO. 2006 Stabilization of a turbulent premixed flame using a nanosecond repetitively pulsed plasma. *IEEE Trans. Plasma Sci.* **34**, 2471–2477. (doi:10.1109/TPS.2006.886081)
12. Kim W, Do H, Mungal MG, Cappelli MA. 2006 Plasma-discharge stabilization of jet diffusion flames. *IEEE Trans. Plasma Sci.* **34**, 2545–2551. (doi:10.1109/TPS.2006.886084)
13. Kim W, Mungal MG, Cappelli MA. 2008 Formation and role of cool flames in plasma-assisted premixed combustion. *Appl. Phys. Lett.* **92**, 051503. (doi:10.1063/1.2841894)
14. Pilla G, Lacoste DA, Veynante D, Laux CO. 2008 Stabilization of a propane-air swirled flame using a nanosecond repetitively pulsed plasma. *IEEE Trans. Plasma Sci.* **36**, 940–941. (doi:10.1109/TPS.2008.927343)
15. Starikovskii AY, Anikin NB, Kosarev IN, Mintoussov EI, Nudnova MM, Rakitin AE, Roupassov DV, Starikovskaia SM, Zhukov VP. 2008 Nanosecond-pulsed discharges for plasma-assisted combustion and aerodynamics. *J. Prop. Power* **24**, 1182–1197. (doi:10.2514/1.24576)
16. Choi I, Uddi M, Zuzeek Y, Adamovich IV, Lempert WR 2009 Stability and heating rate of air and ethylene-air plasmas sustained by repetitive nanosecond pulses. In *Proc. 47th AIAA*

Aerospace Sciences Meeting and Exhibit, Orlando, FL, 5–8 January 2009. Reston, VA: The American Institute of Aeronautics and Astronautics. (doi:10.2514/6.2009-688)

17. Pai D. 2008 Nanosecond repetitively pulsed plasmas in preheated air at atmospheric pressure. PhD thesis, École Centrale Paris, France.
18. Pai DZ, Lacoste DA, Laux CO. 2010 Nanosecond repetitively pulsed discharges in air at atmospheric pressure—the spark regime. *Plasma Sources Sci. Technol.* **19**, 065015. (doi:10.1088/0963-0252/19/6/065015)
19. Rusterholtz DL, Lacoste DA, Pai DZ, Stancu GD, Laux CO. 2013 Ultrafast heating of atmospheric pressure air by nanosecond repetitively pulsed discharges. *J. Phys. D Appl. Phys.* **46**, 464010. (doi:10.1088/0022-3727/46/46/464010)
20. Pilla G. 2008 Etude expérimentale de la stabilisation de flammes de propane-air de pré-mélange par décharge nanosecondes répétitives pulsées. PhD thesis, École Centrale Paris, France.
21. Stancu GD, Simeni Simeni M, Laux CO. 2013 Investigations by Mid-IR QCLAS of pollutant emissions in high temperature exhaust gases released from plasma-assisted combustion. In *Proc. 31st Int. Conf. on Partially Ionized Gases* (*ICPIG*), *Granada, Spain, 14–19 July 2013*, ICPIG paper PS2-117. See http://www.icpig2013.net/papers/556_1.pdf.
22. Lacoste D, Moeck J, Paschereit C, Laux CO. 2013 Effect of plasma discharges on nitric oxide emissions in premixed flame. *J. Propuls. Power* **29**, 748–751. (doi:10.2514/1.B34819)
23. Shkurenkov I, Burnette D, Lempert WR, Adamovich IV. 2014 Kinetics of excited states and radicals in a nanosecond pulse discharge and afterglow in nitrogen and air. *Plasma Sources Sci. Technol.* **23**, 065003. (doi:10.1088/0963-0252/23/6/065003)